APPLIED PHYSICS LETTERS **101**, 013108 (2012)

Spatial-temporally resolved high-frequency surface acoustic waves on silicon investigated by femtosecond spectroscopy

Martin Schubert,[1,a)] Martin Grossmann,[1] Oliver Ristow,[1] Mike Hettich,[1] Axel Bruchhausen,[2] Elaine C. S. Barretto,[1] Elke Scheer,[1] Vitalyi Gusev,[3] and Thomas Dekorsy[1]
[1]*Department of Physics and Center for Applied Photonics, University of Konstanz, Konstanz D-78457, Germany*
[2]*Instituto Balseiro and Centro Atómico Bariloche (CNEA), CONICET, Argentina*
[3]*Institut des Molécules et Matériaux du Mans, UMR CNRS 6283, Université du Maine, 72085 Le Mans, France*

(Received 17 April 2012; accepted 5 June 2012; published online 3 July 2012)

Various types of surface acoustic waves are generated by femtosecond pulses on bulk silicon with aluminium stripe transducers. Rayleigh and leaky longitudinal surface acoustic wave modes are detected in the time domain for various propagation distances. The modes are identified by measuring on various pitches and comparing the spectra with finite element calculations. The lifetimes of the modes are determined quantitatively by spatially separating pump and probe beam, showing a significant difference in the lifetimes of both modes. We were able to excite and measure Rayleigh modes with frequencies of up to 90 GHz using a 100 nm period grating. © *2012 American Institute of Physics*. [http://dx.doi.org/10.1063/1.4729891]

Surface acoustic waves (SAWs) have been of great interest for the last 50 years since the invention of interdigital transducers.[1] While low frequency SAWs in the ultrasonic range have made their success path in communication and signal processing technologies,[2] higher frequency SAWs have found applications in several areas, such as material characterization,[3,4] photonic modulation,[5] phononic crystals,[6] optomechanics,[7] and transport by phonons of other excitations in solids.[8,9] The ability to excite higher acoustic frequencies and identify their correspondent modes is therefore the key to enable further advances in these and other areas. While there are a number of techniques to create SAWs, the highest frequencies achieved so far are by photoacoustic excitation using thin stripe metal transducers on transparent and semi-transparent substrates. The waves are excited by the thermoelastic expansion of the fingers, creating a stress in the material underneath.[10,11]

SAWs with frequencies of up to 50 GHz using nickel stripes on sapphire have been recently obtained by Nelson *et al.*[12] Slightly lower frequencies with aluminum stripes on silicon (Si) were generated by Sadhu *et al.* to investigate the effect of changing the ratio between the period of the grating and finger width.[13] In both cases the waves were excited by pumping a large area of the grating. In our measurements we are locally exciting and probing the SAWs by using small pump and probe spots, and thereby directly measuring propagation distances and the decay of the excited waves up to 90 GHz frequencies. Instead of measuring surface displacement, we detect the change in optical reflectivity due to the strain created by the waves. While other methods have been used to completely map the acoustic band structure of SAWs such as Rayleigh-like waves (RSAW) and leaky longitudinal SAWs (LLSAW),[14] no measurements at such high frequencies have been performed so far that were able to spatially and temporally map these modes.

The samples were fabricated using standard techniques on (001) Si wafers. The process was started by cleaning the samples and spinning a thin layer of PMMA on top. Grating patterns were defined by electron beam lithography and subsequent development. A short reactive ion etching was used to etch a few nanometers (~3 nm) into the material to improve the adhesion of the aluminium (Al) fingers and to generate an initial stress that better matches the profile of the SAWs. Afterwards the Al was evaporated on top and the process was finished by a lift-off to remove the photoresist as well as the Al on top of it, leaving the fingers of the transducers on the surface. The fingers were aligned perpendicularly to the [110] direction.

Samples with five different pitches were fabricated, ranging from a period of 600 nm down to 100 nm in steps of 100 nm. There were no samples with a pitch of 500 nm. Finger widths varied and were typically half the period except in the case of the 600 nm period where it was a third of the period. The fingers have a length of ~80 microns and the entire grating covers a 80 μm by 35 μm area.

The samples were excited and measured using the high-speed asynchronous optical sampling (ASOPS) technique.[15] High-speed ASOPS is a pump probe technique that uses two Ti-Sapphire femtosecond lasers with a repetition rate of 800 MHz. The lasers have an offset in repetition rate of 5 kHz and are locked to each other. Due to the difference in repetition rate, the pulses have a varying time delay without the need of a mechanical delay line. This offers improved stability and, due to the high repetition rate, an improved signal-to-noise ratio compared to conventional pump-probe techniques that use mechanical delay stages.

The pump laser was set to a wavelength of 790 nm and the probe laser to 820 nm. Both lasers have a pulse length of ~50 fs. They are focused onto the sample using a microscope objective with a numerical aperture of 0.55. The probe light polarization is parallel to the grating while the one of the pump is perpendicular. The spot size is resolution limited

a)Electronic mail: martin.schubert@uni-konstanz.de.

with a FWHM of less than 2 μm. The pump and probe powers used were 70 and 5 mW, respectively. The probe pulses are detected using a high-speed 125 MHz photo diode. It is possible to pump and probe at different places on the gratings by spatially displacing the pump spot.

Using the theory developed by Gusev *et al.*[16] and approximating the absorbed power,[17] the strain in the RSAW generated by a grating with a 200 nm period is estimated to be about 10^{-4}. This strain is an order of magnitude higher than reported previously[18] for structures with similar parameters, which is to be expected since the pump laser fluence is also about an order of magnitude larger.

Figure 1 shows time traces of three different measurements on the 600 nm period grating with varying displacements of the pump spot relative to the probe spot. All traces are shifted in time in order to display them in one graph. The signals consist of two dominant sine waves with a Gaussian envelope, corresponding to the two dominant frequencies as shown in the Fourier transform (Fig. 2). The Gaussian envelope is caused by the finite spot size used to excite the grating, i.e., the number of cycles corresponds to the number of Al stripes excited. The decay of the amplitudes for larger propagation distances is clearly observed.

Figure 2 shows the Fourier transform obtained from measurements on four gratings with different periods. In these spectra, pump and probe spots are overlapping. A series of peaks can be seen that shift towards higher frequencies for smaller periods. The spectra for the 100 nm period are plotted separately in Fig. 3 with a different frequency scale. To identify the measured modes, the frequencies of the main peaks for the five different periods are plotted over the nominal periods of the gratings in Fig. 4. Alongside the measurements, the results of finite element simulations are plotted showing a good quantitative agreement to the measured frequencies. The small differences between measured and calculated frequencies are most likely caused by fabrication imperfections of the fingers.

The finite element calculations were performed using COMSOL Multiphysics software.[19] The calculations were based on eigenfrequency analysis assuming a periodic structure. The material constants were taken from Auld,[20] and Euler rotation was applied to the compliance matrix of Si for propagation in the [110] direction. The height of the fingers was kept fixed (14 nm), while the period and the width of the geometry varied, keeping the filling factor of one half, which means that the system does not scale uniformly for different periods, since the height over width ratio of the finger changes (aspect ratio).

The first mode can be identified as a RSAW with the period of the grating corresponding to the wavelength of the mode. The propagation speed of the mode obtained by fitting

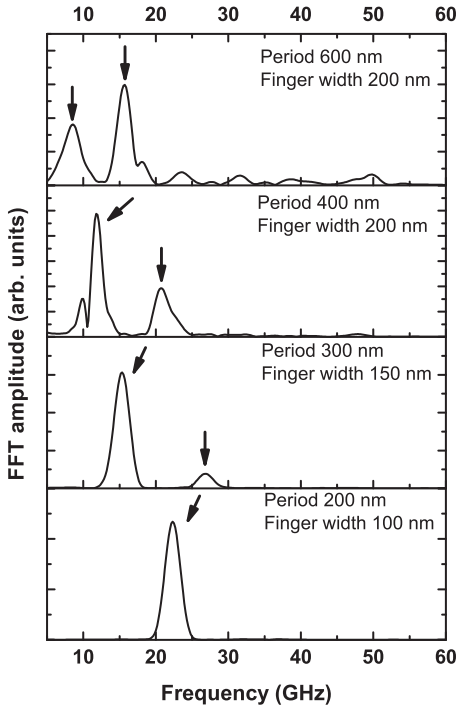

FIG. 2. Spectra of the gratings with periods of 600, 400, 300, and 200 nm. Pump and probe spot were overlapping. Relevant peaks are marked (see text). The first peak corresponds to the RSAW and second peak to the LLSAW. The LLSAW peak is not visible in the last spectrum due to its small intensity.

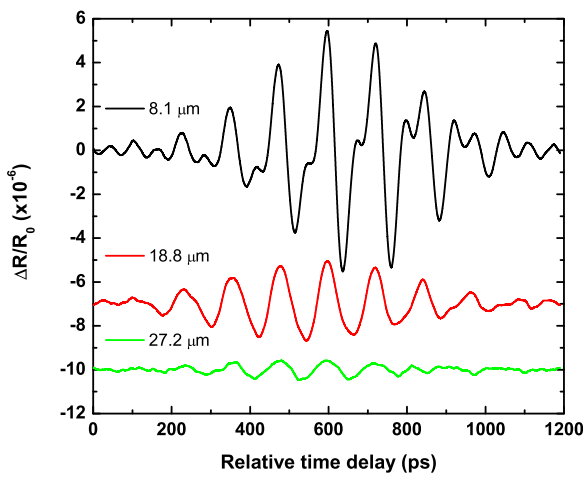

FIG. 1. Extracted oscillations obtained from the transducers with 600 nm period for different distances between pump and probe spot. For better comparability the traces are offset and shifted so that the centers of the gaussian envelopes of the measured sine waves coincide.

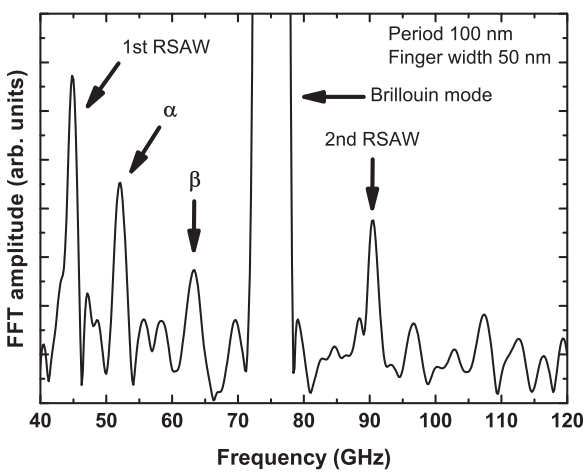

FIG. 3. Spectrum of the grating with a period of 100 nm. Pump and probe are overlapping. Relevant peaks are marked and explained in the text. Note that the frequency scale differs from the other spectra presented in Fig. 2. The large peak in the center of the spectra is caused by the Brillouin mode and only visible when pump and probe overlap.

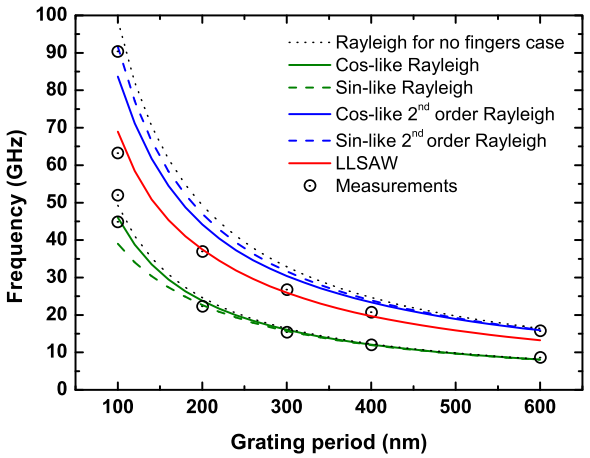

FIG. 4. Frequency over nominal grating period diagram of the measured dominant modes. Measured modes are plotted next to the results of finite element simulations for a large number of different pitches.

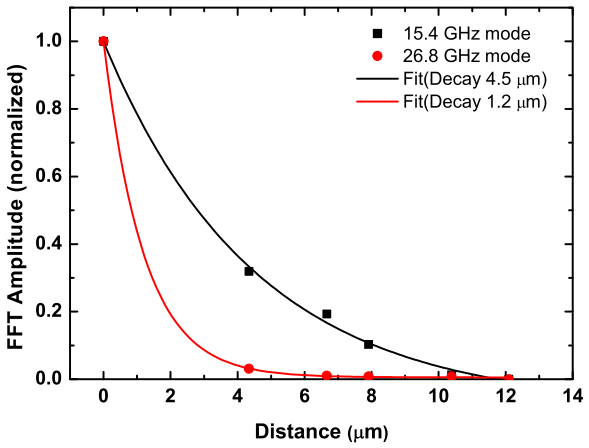

FIG. 5. Decay of the RSAW and LLSAW for the 300 nm period. Each point corresponds to the amplitude of the mode measured with a certain distance between pump and probe in the corresponding spectrum (spectra not shown). Amplitudes are normalized to the peaks in the spectra with overlapping pump and probe spot to better compare the different decay lengths of both modes. Distance between pump and probe was measured by imaging the surface with both spots visible. The fits are exponential decay functions.

the experimental data is 4521 m/s, which is below the speed of the slowest shear bulk wave in the [110] direction of Si (~4670 m/s) as expected for a RSAW.[21] It should be noted though that the speed increases with smaller aspect ratios (larger period) due to the smaller influence of the grating.[22] We confirmed that all of these modes are propagating by doing measurements with a displaced pump spot, which is exemplified in Fig. 1.

It is important to notice that due to the presence of the fingers, the eigensolutions for the Rayleigh mode split into two solutions—a sine-like and a cosine-like one.[22] The difference in frequency between the two solutions is dependent on the geometric and mechanical characteristics of the structure. The calculations for the measured structures show that the two solutions get closer and closer in frequency for smaller aspect ratios of the fingers, approaching the case of the absence of the fingers in which they are degenerate.

At large grating periods the second dominant mode lies close to the position of the 2nd harmonic of the RSAW. Estimating the speeds of the modes shows that they are significantly faster than the RSAW and approach the speed of longitudinal bulk waves (~9000 m/s). We attribute these modes to so called LLSAW that have a dominant longitudinal component and are attenuated mostly because of the emission of bulk shear waves.[14,23,24] The calculated mode patterns for the LLSAW show clear signs of this longitudinal character of the wave (along the surface polarization).

The grating period of 100 nm shown in Fig. 3 is a special case. The height of the stripes approaches the wavelength of the SAW, and therefore the influence of the fingers on the modes becomes larger, leading to a larger splitting between degenerate solutions and also to the appearance of modes which are strongly confined to the metal. We believe that, for this reason, more modes could be detected on this structure. The calculations show that the mode at ~52 GHz (α mode) indicates a pseudo-SAW,[25] while the mode at ~63 GHz (β mode) indicates a vibrational mode of the stripes.[26]

Furthermore we can see a 2nd harmonic RSAW at 90.4 GHz for the 100 nm grating. The numerical calculations also show for this case that a large part of the mode is confined to the fingers. To further quantify the influence of the fingers on the RSAW is beyond the scope of this article, but it appears to allow for the mode to be more efficiently excited/detected in the case of the 100 nm period grating than for the other periods. Measurements indicate that the 2nd harmonic in Fig. 3 significantly decays over a length of less than a micron. Nevertheless it can be detected at distances where pump and probe spot are clearly separated (~5 μm apart) due to the high sensitivity of the ASOPS system ($\Delta R/R_0 \sim 10^{-7}$).

Regarding the 2nd harmonic of the RSAW in the other grating periods, we assume that it is largely suppressed due to the filling factor of our gratings, which is one half for all the different periods, apart as mentioned before in the case of the 600 nm grating, where the filling factor is one third. According to the calculations, the 2nd harmonic for the 600 nm grating lies close in frequency to the LLSAW as can be seen in Fig. 4. In fact all the measurements in Figs. 2 and 3 show that the first peak is larger than the second except in the case of the 600 nm grating where this is reversed. This indicates that the 2nd harmonic RSAW is also present for this period but overlaps with the LLSAW.

Figure 5 shows the FFT amplitudes at various distances between pump and probe of the two dominant modes at 15.4 GHz (RSAW) and 26.8 GHz (LLSAW) measured for a grating with a period of 300 nm and a finger width of 150 nm. The lifetime of the RSAW is determined using the 1/e value of an exponential function fitted to the FFT amplitudes divided by the speed of the RSAW ~4800 m/s. It has a lifetime of ~930 ps, which is similar to values reported earlier.[13] The lifetime of the LLSAW is considerably shorter with ~150 ps at a speed of ~8040 m/s. Both fits are shown in the figure as well as the measured propagation distances. The speeds are calculated by assuming that the wavelength is the same as the period of the grating for both the RSAW and the LLSAW. Due to the presence of the metal fingers, both waves are dispersive as mentioned previously, and therefore these speeds are specific to the grating with a period of 300 nm.

Similar measurements can be carried out for all the gratings, but with smaller periods it becomes increasingly difficult due to the shorter propagation length of the waves and the general quality of the gratings becoming lower due to fabrication issues. For the fast decaying waves the propagation length approaches the spot size, which complicates determining the lifetime of the modes.

In conclusion we have been able to excite and detect RSAW with frequencies of up to 90 GHz in Si. Simultaneously, LLSAWs were detected with frequencies of up to 52 GHz. We measured propagation distances of several microns for SAWs above 10 GHz which allows to design experiments in which one can utilize these waves to probe various nanostructures. By using membranes instead of bulk Si we should be able to excite waves at even higher frequencies. The frequency can also be increased by further reducing the period of the gratings to less than 100 nm which should allow us to generate and detect waves with frequencies beyond 100 GHz.

This work was supported by the DFG through the SFB 767 (Germany) and by the Ministry of Science, Research and Arts of Baden-Württemberg (Germany). A. Bruchhausen thanks the Alexander von Humboldt Foundation (Bonn, Germany) for financial support. We also thank Matthias Hagner for providing support in the cleanroom.

[1]R. M. White and F. W. Voltmer, Appl. Phys. Lett. **7**, 314 (1965).
[2]D. Morgan, *Surface Acoustic Wave Filters: With Applications to Electronic Communications and Signal Processing*, 2nd ed. (Academic, 2007), p. 448.
[3]T. Lee, K. Ohmori, C.-S. Shin, D. G. Cahill, I. Petrov, and J. E. Greene, Phys. Rev. B **71**, 144106 (2005).
[4]P. Hess, Phys. Today **55**(3), 42 (2002).
[5]D. A. Fuhrmann, S. M. Thon, H. Kim, D. Bouwmeester, P. M. Petroff, A. Wixforth, and H. J. Krenner, Nat. Photonics **5**, 605 (2011).
[6]D. Nardi, M. Travagliati, M. E. Siemens, Q. Li, M. M. Murnane, H. C. Kapteyn, G. Ferrini, F. Parmigiani, and F. Banfi, Nano Lett. **11**, 4126 (2011).
[7]G. Bahl, J. Zehnpfennig, M. Tomes, and T. Carmon, Nat. Commun. **2**, 403 (2011).
[8]W. J. M. Naber, T. Fujisawa, H. W. Liu, and W. G. van der Wiel, Phys. Rev. Lett. **96**, 136807 (2006).
[9]O. D. D. Couto, F. Iikawa, J. Rudolph, R. Hey, and P. V. Santos, Phys. Rev. Lett. **98**, 036603 (2007).
[10]C. Thomsen, H. T. Grahn, H. J. Maris, and J. Tauc, Phys. Rev. B **34**, 4129 (1986).
[11]B. Bonello, A. Ajinou, V. Richard, P. Djemia, and S. M. Chérif, J. Acoust. Soc. Am. **110**, 1943 (2001).
[12]M. E. Siemens, Q. Li, M. M. Murnane, H. C. Kapteyn, R. Yang, E. H. Anderson, and K. A. Nelson, Appl. Phys. Lett. **94**, 093103 (2009).
[13]J. Sadhu, J. H. Lee, and S. Sinha, Appl. Phys. Lett. **97**, 133106 (2010).
[14]D. M. Profunser, O. B. Wright, and O. Matsuda, Phys. Rev. Lett. **97**, 055502 (2006).
[15]A. Bartels, R. Cerna, C. Kistner, A. Thoma, F. Hudert, C. Janke, and T. Dekorsy, Rev. Sci. Instrum. **78**, 035107 (2007).
[16]V. Z. Gusev and A. A. Karabutov, *Laser Optoacoustics*, 1st ed. (American Institute of Physics, 1992), p. 336.
[17]D. Zhang, P. Wang, X. Jiao, C. Min, G. Yuan, Y. Deng, H. Ming, L. Zhang, and W. Liu, Appl. Phys. B: Lasers Opt. **85**, 139 (2006).
[18]D. H. Hurley, R. Lewis, O. B. Wright, and O. Matsuda, Appl. Phys. Lett. **93**, 113101 (2008).
[19]COMSOL Software, version 4.2a), 2012, Retrieved from http://www.comsol.com/.
[20]B. A. Auld, *Acoustic Fields and Waves in Solids* (Krieger Pub Co, 1990).
[21]R. G. Pratt and T. C. Lim, Appl. Phys. Lett. **15**, 403 (1969).
[22]N. E. Glass, R. Loudon, and A. A. Maradudin, Phys. Rev. B **24**, 6843 (1981).
[23]N. E. Glass and A. A. Maradudin, J. Appl. Phys. **54**, 796 (1983).
[24]O. Holmgren, J. V. Knuuttila, T. Makkonen, K. Kokkonen, V. P. Plessky, W. Steichen, M. Solal, and M. M. Salomaa, Appl. Phys. Lett. **86**, 024101 (2005).
[25]T. C. Lim and G. W. Farnell, J. Acoust. Soc. Am. **45**, 845 (1969).
[26]H.-N. Lin, H. J. Maris, L. B. Freund, K. Y. Lee, H. Luhn, and D. P. Kern, J. Appl. Phys. **73**, 37 (1993).